

Effects of Ar/O₂ Gas Ratio on the Properties of the Zn_{0.9}Cd_{0.1}O Films Prepared by DC Reactive Magnetron Sputtering

I. SHTEPLIUK^{a,*}, G. LASHKAREV^a, V. KHOMYAK^b, P. MARIANCHUK^b, P. KORENIUK^c,
D. MYRONIUK^a, V. LAZORENKO^a AND I. TIMOFEEVA^a

^aI. Frantsevich Institute for Problems of Material Science, NASU, 03680, Kiev-142, Ukraine

^bChernivtsi National University, 58012, Chernivtsi, Ukraine

^cInstitute of Physics, NASU, 03028, Kiev, Ukraine

Zn_{0.9}Cd_{0.1}O ternary alloys have been grown on the sapphire substrates by using the direct current (dc) magnetron sputtering. X-ray diffraction measurements showed that all samples were highly oriented films along the *c*-axis perpendicular to the substrate surface. X-ray diffraction confirmed that the crystal quality of Zn_{0.9}Cd_{0.1}O films can be controlled by changing the gas ratio of Ar/O₂. The optical properties of these films have been investigated by means of the optical transmittance and the low-temperature photoluminescence spectra. It was found that the optical band gap of the deposited films can be tuned by growth parameters. The luminescence processes are considered in the terms of alloy fluctuation.

PACS: 78.55.Et, 78.67.Bf

1. Introduction

In the last years, great progress has been made in the optoelectronics with blue and green light-emitting diodes for the high-density optical storage and devices for high-power applications, which can operate over a wide temperature range and are resistant to the corpuscular irradiation. Experimental and theoretical studies have been addressed to the extraordinary optical properties of the zinc oxide relevant to such applications. ZnO with a wide band gap of 3.37 eV and an exciton binding energy of 60 meV is under intensive investigation for its potential use in blue and ultraviolet (UV) optoelectronic devices [1, 2]. Recently, many groups have fabricated homojunction or heterojunction prototypes of light-emitting diodes (LEDs) based on ZnO and realized their electroluminescence (EL) [3]. In order to construct optical and electrical confinement structures, a quantum well material with smaller band gap has to be proposed. The ZnCdO alloy is one of the most promising quantum well materials because its lattice constant is very close to that of the ZnO. Therefore, the carriers and the photons can be confined in the ZnO/ZnCdO/ZnO quantum well.

In the present work, high-transparent Zn_{0.9}Cd_{0.1}O films were deposited by DC reactive magnetron sputtering. The dependence of the structural properties of

Zn_{0.9}Cd_{0.1}O films on the gas ratio of Ar/O₂ has been studied. The optical properties of the films at the different gas ratios have been investigated systematically by using the optical transmittance and the low-temperature photoluminescence (LT PL) measurements.

2. Experimental details

The Zn_{0.9}Cd_{0.1}O films were grown by the dc magnetron sputtering on the sapphire *c*-Al₂O₃ substrates at the temperature of 250 °C. A disc of 90%zinc–10%cadmium alloy of 100 mm diameter with a purity of 99.99% was used as a target. High purity argon and oxygen were used as the sputtering and the reactive gas, respectively. The target-to-substrate distance was 40 mm. The chamber was pumped to a base pressure of 1×10^{-4} Pa before deposition. The films were grown in the ambient with the Ar/O₂ ratios ranging from 2:1 to 4:1. The dc power was maintained at 150 W. The crystal structure of the samples was investigated by XRD method, where a Cu K_{α} ($\lambda = 0.154056$ nm) source was used. The XRD measurements were carried out with the DRON-4 system. The transmittance measurements were performed by a SF-2000 spectrophotometer. Photoluminescence of the Zn_{0.9}Cd_{0.1}O films was studied at the temperatures of 4.2 K and 77 K by an Acton 2500i monochromator with a CCD camera. The third harmonic of a femtosecond Ti:sapphire laser (266 nm, 37 mW, 170 fs, 76 MHz) was used as excitation source.

* corresponding author; e-mail: shteplyuk_1987@ukr.net

At this study, energy pumping density per pulse P was fixed at 2.5 nJ/cm^2 . It should be noted that photons with $\lambda = 266 \text{ nm}$ ($h\nu = 4.67 \text{ eV}$) at excitation by the third harmonic of Ti:sapphire laser are strongly absorbed in ZnCdO. Scanning electron microscopy (SEM) was used to reveal the uniformity of the films and the quality of the film/substrate interface (ZEISS EVO 50 XVP). An acceleration voltage was fixed at 20 kV . An elemental analysis of the ZnCdO films was also done by ZEISS EVO 50 XVP SEM using energy dispersive X-ray spectroscopy (EDXS) furnished INCA 450 (Oxford Instruments). An operating voltage for EDXS analysis on the Oxford is 20 kV .

3. Results and discussions

Figure 1 shows XRD patterns of the $\text{Zn}_{0.9}\text{Cd}_{0.1}\text{O}$ films grown on the c -plane sapphire substrates. Diffraction peaks of (002) and weak peaks of (004) from the $\text{Zn}_{0.9}\text{Cd}_{0.1}\text{O}$ phase were observed. It should be noted that no diffraction peaks corresponding to CdO or other additional phases were observed. These results indicate that the $\text{Zn}_{0.9}\text{Cd}_{0.1}\text{O}$ films are of hexagonal wurtzite

structure with pronounced c -axis orientation. The c -axis orientation is believed to result from the lowest surface energy of the (001) basal plane in ZnCdO, thus leading to a preferred growth in the c -axis. Results of the XRD analysis are presented in Table I.

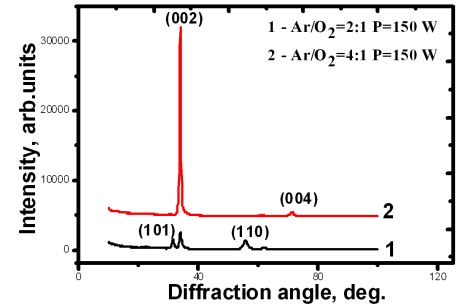


Fig. 1. XRD patterns of $\text{Zn}_{0.9}\text{Cd}_{0.1}\text{O}$ ternary alloys deposited at the different growth conditions.

XRD data for $\text{Zn}_{0.9}\text{Cd}_{0.1}\text{O}$ films grown by the dc magnetron sputtering.

TABLE I

Sample	Diffraction angle θ_{002} [deg]	FWHM [deg]	Grain size D [nm]	Lattice period c [Å]
$\text{Zn}_{0.9}\text{Cd}_{0.1}\text{O}$ (150 W, 2:1)	33.99	1.103	7	5.270
$\text{Zn}_{0.9}\text{Cd}_{0.1}\text{O}$ (150 W, 4:1)	33.96	0.525	16	5.275

When increasing the Ar/ O_2 gas ratio from 2:1 to 4:1, the value of the FWHM is decreased whereas the size of coherent scattering areas (grain sizes) for the films, grown at higher argon concentration in the gas mixture of Ar- O_2 , is increased. Thus, the film grown at the Ar/ O_2 ratio of 4:1 is more structurally ordered than the film grown at the gas ratio of 2:1. Additionally, at the increase of the argon concentration in a mixture Ar- O_2 , the lattice period in $\text{Zn}_{1-x}\text{Cd}_x\text{O}$ increases. It can be explained as follows. By using the DC reactive magnetron sputtering, the Cd and Zn atoms supplied by the target are fixed per unit of time. Different Ar/ O_2 gas ratios corresponding to different saturated vapor pressures and cadmium is more active than zinc when it reacts with oxygen. With the increase in Ar/ O_2 gas ratios, the argon partial pressure is increased and the sputtering yield is enhanced, so cadmium can react more easily with oxygen. Thus, more cadmium atoms can replace zinc atoms and reach crystal lattice sites.

Figure 2a shows transmittance curves for the $\text{Zn}_{1-x}\text{Cd}_x\text{O}$ films, where the films due to interference phenomena between the wave fronts generated at the

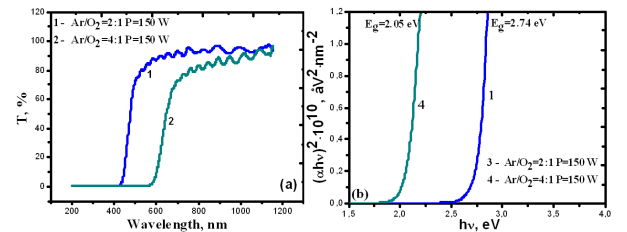


Fig. 2. Optical transmittance spectra (a) and dependences of $(\alpha h\nu)^2$ vs. $h\nu$ (b) for the $\text{Zn}_{0.9}\text{Cd}_{0.1}\text{O}$ films, deposited on the sapphire substrates at the different gas ratios.

two interfaces (air and substrate) defines the sinusoidal behavior of the curves' transmittance vs. wavelength of light. ZnCdO films showed interference fringe pattern in transmission spectrum. This revealed the smooth reflecting surfaces of the films and there was not much scattering loss at the surface. In transparent metal oxides, metal to oxygen ratio decides on the percentage of transmittance. A metal rich film usually exhibits less

transparency. The excellent surface quality of the film was confirmed from the appearance of interference fringes in the transmission spectra. This occurs when the film surface is reflecting without much scattering/absorption in the bulk of the film. The film exhibited good transparency in the visible region ($\approx 80\%$). The absorption coefficient α of the ZnCdO films was determined from transmittance measurements. Since envelope method is not valid in the strong absorption region, the calculation of the absorption coefficient of the films in this region was calculated using the following expression:

$$\alpha(\nu) = 2.303A/t, \quad (1)$$

where A is the optical absorbance. The optical absorption edge was analyzed by the following equation [4]:

$$\alpha h\nu = B(h\nu - E_g)^{0.5}, \quad (2)$$

where B is a constant. The variation of $(\alpha h\nu)^2$ with photon energy $h\nu$ for the ZnCdO film is shown in Fig. 2b. It has been observed that the plot of $(\alpha h\nu)^2$ versus $h\nu$ is linear over a wide range of photon energies indicating the direct type of transitions. The extrapolations of these plots on the energy axis give the energy band gap. At the Ar/O₂ ratios of 2:1 and 4:1, the optical band gap of the Zn_{0.9}Cd_{0.1}O films are 2.74 eV and 2.05 eV, respectively. The bandgap shift in the low-energy region of the spectrum indicates that more cadmium ions can substitute zinc ions in a cationic sublattice of the zinc oxide. The difference in the band gaps among these films can be explained as follows. Since Cd has a larger Bohr radius than Zn, the incorporation of Cd into ZnO crystal lattice may introduce lattice distortion in the ZnO film. After all, Cd doping into ZnO influences the energy structure of ZnO and thus a new band structure may be formed, which should result in changes of the band gap. Therefore, larger number of cadmium will lead to large changes in the band gap.

It is also assumed that the absorption coefficient near the band edge shows an exponential dependence on the photon energy and this dependence is given as follows [4]:

$$\alpha h\nu = \alpha_0 \exp\left(\frac{h\nu}{E_u}\right), \quad (3)$$

where α_0 is a constant and E_u is the Urbach energy interpreted as the width of the tails of localized states, associated with the amorphous state, in the forbidden gap. The $\ln(\alpha)$ vs. photon energy plots for the ZnCdO film is shown in Fig. 3. With the increase in the Ar/O₂ gas ratio from 2:1 to 4:1, the Urbach energy decreases from 155 meV to 141 meV. The change of the Urbach energy can be attributed to the change of the crystallinity. At the Ar/O₂ gas ratio of 4:1, the film has the narrowest value of FWHM, that is, it has the best crystal quality, so the Urbach energy of the film is much smaller than that of the films prepared at other gas ratios.

Figure 4 shows the low temperature PL spectra collected at the temperatures of 4.2 K and 77 K. The Zn_{0.9}Cd_{0.1}O ($P = 150$ W, Ar/O₂ $\approx 4:1$) film char-

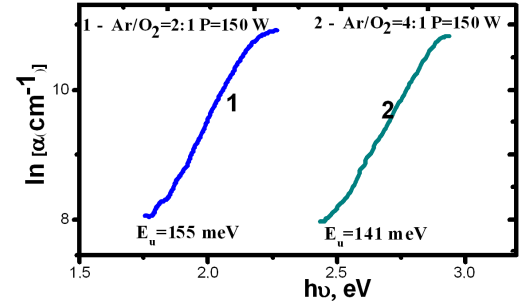


Fig. 3. Urbach plots of the Zn_{0.9}Cd_{0.1}O film grown at the different gas ratios.

acterized by the ultraviolet PL emission peak at the 3.359 eV and a donor–acceptor pair emission peak located at 3.305 eV, which implies a number of donors and acceptor bounded excitons existing in the ZnCdO crystallites (Fig. 4). The appearance of these distinguished emission peaks can be probably related with the presence of the Cd-poor regions of the film. The near band edge PL emission of the ZnCdO is only dominated by the bounded excitons at 4.2 K. At the temperature of 77 K, the peaks at 3.359 eV and 3.305 eV, that were predominant at 4.2 K, disappear. This is interpreted as the unbinding of exciton with increasing thermal energy.

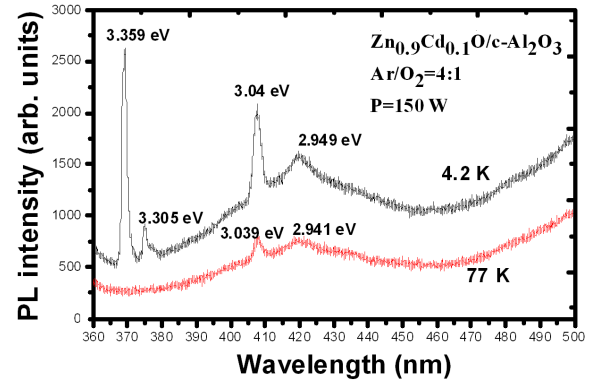


Fig. 4. Low-temperature PL spectra for the ZnCdO ternary alloys deposited at the Ar/O₂ gas ratios of 4:1 and magnetron power of 150 W.

Many groups have intensively studied the lines at the 3.359 eV and 3.305 eV. Meyer et al. [5] assigned line at 3.359 eV to donor bound exciton recombination (D^0X), where gallium plays a role of the donor. Zaleszczyk et. al. [6] have believed that the emission peak at 3.359 eV originated from the radiative recombination of acceptor-bound excitons (A_0X). This line is inhomogeneously broadened due to the overlapping of several lines related to various acceptors. The FWHM of the dominant line is ≈ 14 meV at 4.2 K. The peak at 3.305 eV has been ascribed to donor–acceptor pair (DAP) emission, which is identified as transitions of electrons in the donor states with holes localized at relatively shallow acceptor states,

which are associated with basal plane stacking faults [7].

For $\text{Zn}_{0.9}\text{Cd}_{0.1}\text{O}$ film, the exciton emission shifts to lower energy with increasing temperature. It can be explained as follows. The main characteristics of localized excitonic emission are seen in the emission energy dependence of the emission lifetime. At low temperatures, where excitons occupy localized states, the emission lifetime of the high-energy side of the localized excitonic emission band is short, and becomes longer as the emission band shifts to lower energies [8]. With increasing temperature, excitons undergo transitions from localized to delocalized states due to thermal energy, with decreasing differences of emission lifetimes in the low and high-energy regions. At high temperatures, the excitons become totally delocalized and the emission lifetimes are the same for all bands. At the temperatures of 4.2 K and 77 K, in the $\text{Zn}_{0.9}\text{Cd}_{0.1}\text{O}$ samples two separate luminescence bands can be clearly distinguished with emission energies of 3.04 eV and 2.94 eV, respectively. The appearance of the low-energy and high-energy peaks gives an evidence of a possible existence of the second Cd-rich region which would correspond to higher cadmium content. It can be explained by the alloy fluctuation. Thus, we have the main Cd poor region corresponding to the average Cd-composition and a second minor Cd-rich region. In order to verify or falsify this assumption we performed the scanning electron microscopy and energy-dispersive X-ray spectroscopy.

Figure 5 shows the SEM image of the $\text{Zn}_{0.9}\text{Cd}_{0.1}\text{O}$ film cross-section. We have chosen the four different points in a cross-section plane and the EDX spectra along the line of the selected area were obtained for each point.

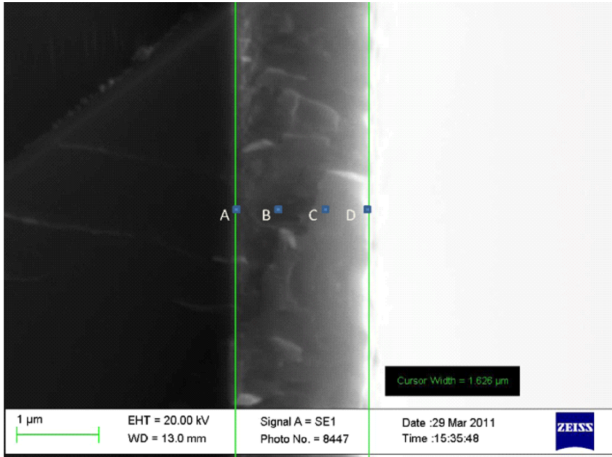


Fig. 5. SEM image of the ZnCdO film cross-section.

The results of the EDX studies are presented in Table II. These results show that the different regions of the ZnCdO film are characterized by the different cadmium content, thereby indicating the existence of the Cd-rich and Cd-poor regions. Morrison et al. [9] reported the similar results for the $\text{Mg}_x\text{Zn}_{1-x}\text{O}$ films, grown via a chemical approach. There was shown a similar trend

in the PL characteristics for these ternary alloys at the phase separation range. Specifically, the PL spectra of the $\text{Mg}_{0.4}\text{Zn}_{0.6}\text{O}$ were found to have multiple emission lines: the low energy ones corresponding to the Zn-rich of the wurtzite structure, and the higher energy ones corresponding to the Mg-rich.

TABLE II

Data of the energy dispersive X-ray spectroscopy for the $\text{Zn}_{0.9}\text{Cd}_{0.1}\text{O}$ film collected in the mode of line profile analysis.

Spectrum along the line	Elemental content [at.%]		
	Zn	O	Cd
A	84.97	5.84	9.19
B	77.84	12.38	9.78
C	62.86	24.91	12.23
D	50.95	41.86	7.19

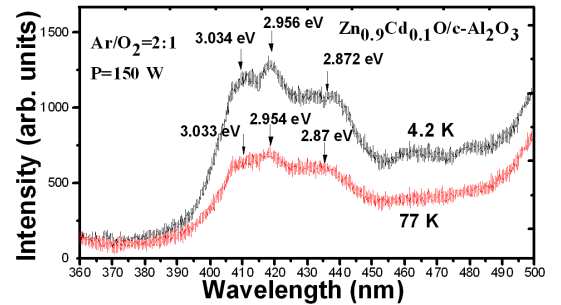


Fig. 6. Low-temperature PL spectra for the $\text{Zn}_{0.9}\text{Cd}_{0.1}\text{O}$ ternary alloy deposited at the Ar/O_2 gas ratios of 2:1 and the magnetron power of 150 W.

With the reduction of the argon concentration in an $\text{Ar}-\text{O}_2$ mixture, the PL spectra of the $\text{Zn}_{0.9}\text{Cd}_{0.1}\text{O}$ significantly differ from the PL spectra of ternary alloy deposited at the gas ratio of 4:1 (Fig. 6). It is due to the deterioration of the structural quality of this ternary alloy (Table I, Fig. 3). The low-temperature (4.2 K) PL spectrum of the $\text{Zn}_{0.9}\text{Cd}_{0.1}\text{O}$ ($P = 150$ W, $\text{Ar}/\text{O}_2 \approx 2:1$) is characterized by the broad band (400–450 nm), which results from the superposition of three exciton lines of 2.872 eV, 2.956 eV, and 3.034 eV. The broadening of PL band is related to random alloy fluctuations [10, 11]. For ZnCdO solid solutions, local fluctuations in the composition happen on a microscopic scale due to random occupation on the cation sublattice where the cation sites are occupied by zinc atoms or by cadmium atoms. In the case of ZnO , the exciton Bohr radius is about 2 nm and inside the small excitonic volume, there are less than one thousand cation sites. For such a small number of sites, the fluctuations in the composition are high. As the temperature is increased, the PL peaks for $\text{Zn}_{0.9}\text{Cd}_{0.1}\text{O}$ alloys are red-shifted. It can be interpreted as energy transfer from a shallower state to a deeper state as one

would expect for a delocalization effect. At the low temperatures, all the excitons are localized in the depths of the potential. As the temperature is increased, the excitons can escape from the shallower potential fluctuations; they can reach the free exciton continuum, or they can fall into deeper fluctuations.

4. Conclusions

We have grown the Zn_{0.9}Cd_{0.1}O films sapphire substrates by using a dc magnetron sputtering method at the different gas ratios. The Zn_{0.9}Cd_{0.1}O films were preferentially oriented along the *c*-axis. The grain size along the growth direction increased with the increasing of argon concentration in the mixture of Ar-O₂. A strong shift of the absorption edge and a gradual decrease of the optical band gap were observed for Zn_{0.9}Cd_{0.1}O films at the higher gas ratios. The optical transmission studies indicated that the Zn_{0.9}Cd_{0.1}O film (gas ratio of 4:1, *P* = 150 W) has a room-temperature band gap of ≈ 2.05 eV, while that of the ZnO film is at ≈ 3.37 eV; thus in that regard bandgap engineered optical alloy was realized. We have presented low-temperature photoluminescence studies of the Zn_{0.9}Cd_{0.1}O films. Luminescence processes were considered in the terms of alloy fluctuation and delocalization effect of excitons.

References

- [1] Y. Segawa, A. Ohtomo, M. Kawasaki, H. Koinuma, Z.K. Tang, P. Yu, G.K.L. Wong, *Phys. Status Solidi B* **202**, 669 (1997).
- [2] D.M. Bagnall, Y.F. Chen, Z. Zhu, T. Yao, M.Y. Shen, T. Goto, *Appl. Phys. Lett.* **73**, 1038 (1998).
- [3] S.J. Jiao, Z.Z. Zhang, Y.M. Lu, D.Z. Shen, B. Yao, J.Y. Zhang, B.H. Li, D.X. Zhao, X.W. Fan, Z.K. Tang, *Appl. Phys. Lett.* **81**, 1830 (2006).
- [4] F. Urbach, *Phys. Rev.* **92**, 1324 (1953).
- [5] B.K. Meyer, H. Alves, D.M. Hofmann, W. Kriegseis, D. Forster, F. Bertram, J. Christen, A. Hoffmann, M. Strassburg, M. Dworzak, U. Haboeck, A.V. Rodina, *Mater. Sci. Eng. B* **241**, 231 (2004).
- [6] W. Zaleszczyk, K. Fronc, M. Aleszkiewicz, W. Paszkowicz, J. Wróbel, P. Dłuzewski, S. Kret, M. Klepka, A. Kłopotowski, G. Karczewski, T. Wojtowicz, *Acta Phys. Pol. A* **112**, 357 (2007).
- [7] M. Schirra, R. Schneider, A. Reiser, G.M. Prinz, M. Feneberg, J. Biskupek, U. Kaiser, C.E. Krill, K. Thonke, R. Sauer, *Phys. Rev. B* **77**, 125215 (2008).
- [8] Y. Kawakami, M. Funato, Sz. Fujita, Sg. Fujita, Y. Yamada, Y. Masumoto, *Phys. Rev. B* **50**, 14655 (1994).
- [9] J.L. Morrison, J. Huso, H. Hoeck, E. Casey, J. Mitchell, M.G. Norton, L. Bergman, *J. Appl. Phys.* **104**, 123519 (2008).
- [10] O. Goede, L. Johan, D. Henning, *Phys. Status Solidi B* **89**, K183 (1978).
- [11] A. Lusson, R. Legros, Y. Marfaing, H. Mariette, *Solid State Commun.* **67**, 851 (1988).